ELSEVIER

Biophysical Chemistry 88 (2000) 153–163

Biophysical Chemistry

www.elsevier.nl/locate/bpc

Phase-fluorimetry study on dielectric relaxation of human serum albumin

Andrea Buzády[a,b,*], János Erostyák[a,c], Béla Somogyi[b,d]

[a] *Department of Experimental Physics, Institute of Physics, University of Pécs, H-7624 Pécs, Ifjúság u. 6., Hungary*
[b] *Department of Biophysics, University of Pécs, H-7625 Pécs, Szigeti út 12., Hungary*
[c] *Jobin-Yvon Molecular Luminescence Reference Laboratory, University of Pécs, H-7624 Pécs, Ifjúság u. 6., Hungary*
[d] *Research Group of the Hungarian Academy of Sciences at the Department of Biophysics, H-7625 Pécs, Szigeti út 12., Hungary*

Received 5 June 2000; received in revised form 11 September 2000; accepted 13 September 2000

Abstract

The dielectric relaxation (DR) of human serum albumin (HSA) was studied by the method of phase-fluorometry. The protein environment of the single tryptophan in HSA shows a relatively low-speed DR of sub-ns characteristic time. This relaxation can be measured as a decaying red-shift of the time-resolved fluorescence emission spectra. The details of calculations of time–emission matrices (TEM) and comparison to the fluorescence data of the reference solution of *N*-acetyl-L-tryptophanamide (NATA) are also presented.

Keywords: Dielectric relaxation; Human serum albumin; Phase-fluorometry; Time–emission matrix

1. Introduction

The measurement of time-dependent Stokes-shift of a fluorophore provides useful information about the dielectric relaxation phenomena. It is widely used especially to study the solvation relaxation [1–6]. In a protein matrix the dielectric relaxation of the tryptophan (Trp) group's environment can be monitored by the mean of time-resolved fluorescence measurements [7–21].

Proteins often show non-exponential fluorescence decays [22–29], which can be interpreted in more ways. This non-exponentiality can be a consequence of dielectric relaxations, excited state reactions, heterogeneity of Trp groups being in different conformer states, harmonic conforma-

* Corresponding author. Department of Experimental Physics, Institute of Physics, University of Pécs, H-7624 Pécs, Ifjúság u. 6, Hungary. Tel.: +36-72-327622/4488; fax: +36-72-501571.

E-mail address: buzady@fizika.ttk.pte.hu (A. Buzády).

0301-4622/00/$ - see front matter
PII: S0301-4622(00)00210-6

tional fluctuations of the protein, etc. The picture is even more complicated in more Trp-containing proteins [22], in which fluorescence quenching [30], energy transfer, etc., may play an important role in forming the fluorescence decay measured.

The resulted non-exponential fluorescence decay can be fitted by both discrete or continuous distributions of lifetime components [17–21,27,28], reflecting the model chosen. But generally, using three or more exponential components in the fitting procedure, the data measured can be fitted well within the measurements' errors, thus many times the fitting parameters cannot be used to make significant distinctions between the possible background processes. Almost the same decay curves can be obtained using quite different numeric values of lifetime components and pre-exponentials. In this work we will not attribute any quantitative meaning of these numbers characterizing the decays of fluorescence emission at different wavelengths, they just are tools to describe the true shape of the fluorescence decay.

Before a photoexcitation, the fluorophore group is in equilibrium with its surroundings. After the excitation, if the excited state dipole moment differs from that of the ground state, the fluorescence emission start from a non-equilibrium state. Then the protein matrix around the Trp group adjusts its charge distribution until it reaches the equilibrium excited state. This relaxation appears in the fluorescence as a time-dependent red shift, which serves as an instantaneous measure of energy difference between the ground and excited electronic states. [4,5,14]

The one Trp-containing human serum albumin (HSA) was the sample of our investigations. HSA is the principal carrier of fatty acids in the blood and the details of ligand binding to HSA have been studied for decades. There are three structurally homologous domains that repeat in HSA [31]. Each domain is formed by two smaller subdomains. The Trp residue is located in the hydrophobic pocket of the IIA subdomain. Trp plays an important role in the formation of the IIA binding site by limiting the solvent accessibility, and it also participates in a hydrophobic packing interaction between the IIA and IIIA interface. The Trp's fluorescence emission is affected by both the surrounding protein matrix and the solvent's molecules. Both fluorescence emission and dielectric relaxation has components not only in the fs, but the ps–ns time scales, which is detectable with our phase fluorometer. We investigated the influence of solvent's constituents and temperature to the decays of both the fluorescence emission and dielectric relaxation.

2. Materials and methods

2.1. Materials

HSA and NATA were obtained from Sigma and used without further purification.

When measuring aqueous solutions the solutes were dissolved in 0.05 M sodium phosphate buffer (pH = 7.0). In the case of more viscous solution the solvent was 50% (w/w) glycerol/buffer.

To maximize the emission intensity the concentration of the HSA (69 kDa) was set at 5 mg/ml (7.24×10^{-5} M). The molar concentration of solutions of NATA were the same. In time-resolved measurements the reference solution was glycogen in water. Solutions of HSA, NATA and glycogen were prepared freshly.

2.2. Steady-state fluorescence and phase-fluorometry measurements

The fluorescence measurements were carried out by a Jobin-Yvon Fluorolog τ3 fluorometer. It has a double monochromator at the excitation side and a single monochromator at the emission side. In the steady-state mode it works with a single photon counting technique, in the time-resolved operation it works as a phase-fluorometer. The modulation frequency can be set between 0.1 and 310 MHz.

The spectral resolution of the steady-state spectra was 1 nm. In phase-fluorimetry measurements the spectral resolution of the monochromators were:

Excitation monochromator: 2 nm.
Emission monochromator: 20 nm.

In the cases of both steady-state and time-resolved fluorescence measurements regular 1 × 1-cm quartz cuvettes were used. To avoid fluorescence of tyrosine the excitation wavelength of 295 nm was chosen. The 5-mg/ml concentration of HSA means a relatively strong absorption, thus front face (FF) excitation–emission geometry was used.

2.3. Data analysis

The time evolution of the fluorescence emission spectrum due to dielectric relaxation is characterized by the Stokes shift response function $S(t)$:

$$S(t) = \frac{\bar{\nu}(t) - \bar{\nu}(\infty)}{\bar{\nu}(0) - \bar{\nu}(\infty)}, \tag{1}$$

where

$$\bar{\nu}(t) = \frac{\int I(\nu,t)\nu \, d\nu}{\int I(\nu,t) d\nu} \tag{2}$$

is the first moment of the emission spectrum at some time. $I(\nu,t)$ stands for the fluorescence intensity at wavenumber ν and time t. $\bar{\nu}(t)$ is the mean wavenumber of the spectrum.

The emission spectra are measured at equidistant points in the wavelength space, thus the first moment should be calculated as:

$$\bar{\nu}(t) = \frac{\int I(\lambda,t)\lambda^{-3} d\lambda}{\int I(\lambda,t)\lambda^{-2} d\lambda}, \tag{3}$$

where $I(\lambda,t)$ stands for the fluorescence intensity at wavelength λ and time t. The temporal evolution of the dielectric relaxation was calculated by fitting $\bar{\nu}(t)$ and not $S(t)$, thus neglecting the need of assumptions for the unknown value of $\nu(\infty)$:

$$\bar{\nu}(t) = \bar{\nu}(\infty) + [\bar{\nu}(0) - \bar{\nu}(\infty)]S(t) = \bar{\nu}(\infty) + [\bar{\nu}(0) - \bar{\nu}(\infty)] \sum_i a_i e^{-t/\tau_{DRi}} = \bar{\nu}(\infty) + \sum_i b_i e^{-t/\tau_{DRi}}. \tag{4}$$

τ_{DRi} stand for the lifetime components of dielectric relaxation, a_i stand for the pre-exponentials in $S(t)$ and, b_i stand for the pre-exponentials in $\bar{\nu}(t)$. From Eq. (4) it is obvious that

$$\frac{a_i}{a_j} = \frac{b_i}{b_j}. \tag{5}$$

To be able to calculate $\bar{\nu}(t)$ we have to know the time–emission matrix (TEM) of the fluorescence emission. Steps to be performed when calculating $\bar{\nu}(t)$from phase-fluorimetry data:

1. Measurement of phase and modulation data at several emission wavelengths.
2. Calculation of shapes of decay curves by multi-exponential fitting (generally not more than three discrete lifetime components could give proper fit).
3. Calculation of TEM from decay curves and the steady-state emission spectrum.
4. Calculation of $\bar{\nu}(t)$.

Details of 2, and 3.

The time-integrals of the elements of TEM $[I(\nu,t)]$ give the data of integrated fluorescence spectrum $[I_{IFS}(\nu)]$ measured after a short enough excitation:

$$I_{IFS}(\nu) = \int_0^\infty I(\nu,t)\, dt = \int_0^\infty I(\nu,0) f(\nu,t)\, dt, \tag{6}$$

where $I(\nu,0)$ is the fluorescence spectrum at time zero, $f(\nu,t)$ is the decay curve at wavenumber ν normalized to unity. This decay can be written in terms of exponentials:

$$f(\nu,t) = \frac{\sum_i a_i(\nu) e^{-t/\tau_i}}{\sum_i a_i(\nu)} \quad \text{(discrete lifetime components)} \tag{7}$$

or

$$f(\nu,t) = \frac{\int_0^\infty a(\upsilon,\tau)\mathrm{e}^{-t/\tau}\,\mathrm{d}\tau}{\int_0^\infty a(\nu,\tau)\,\mathrm{d}\tau}$$

(continuous distribution of lifetime components). (8)

From Eq. (6) the fluorescence emission spectrum at time zero:

$$I(\nu,0) = \frac{I_{\mathrm{IFS}}(\nu)}{\int_0^\infty f(\nu,t)\,\mathrm{d}t}. \quad (9)$$

Thus, the elements of TEM $[I(\nu,t) = I(\nu,0)f(\nu,t)]$ can be calculated from the integrated fluorescence spectrum and the shapes of decay curves:

$$I(\nu,t) = \frac{I_{\mathrm{IFS}}(\nu)f(\nu,t)}{\int_0^\infty f(\nu,t)\,\mathrm{d}t}. \quad (10)$$

The $I_{\mathrm{IFS}}(\nu)$ is received from steady-state measurements.

The $\bar{\tau}$ average lifetime is also an illustrative parameter characterizing the fluorescence emission at different wavelengths:

$$\bar{\tau}(\nu) = \frac{\int I(\nu,t)\,t\,\mathrm{d}t}{\int I(\nu,t)\,\mathrm{d}t}. \quad (11)$$

When the fluorescence decay is to be written in the terms of exponentials, $\bar{\tau}$ can be calculated as:

$$\bar{\tau}(\nu) = \frac{\sum_i a_i\tau_i^2}{\sum_i a_i\tau_i}. \quad (12)$$

3. Results

3.1. Steady-state spectra

The emission spectrum of HSA is temperature-dependent. At lower temperatures the spectra are slightly blue-shifted (Fig. 1) compared to those measured at higher temperature. Decreasing the temperature from 37 to 2°C the mean emission wavelength decreases by 4 nm in glycerol solution and by 2 nm in buffer solution. Moreover, the emission spectra of solutions containing glycerol are blue-shifted compared to emission spectra of solutions containing buffer by 3–5 nm (depending on the temperature). These observations — in agreement with time-resolved

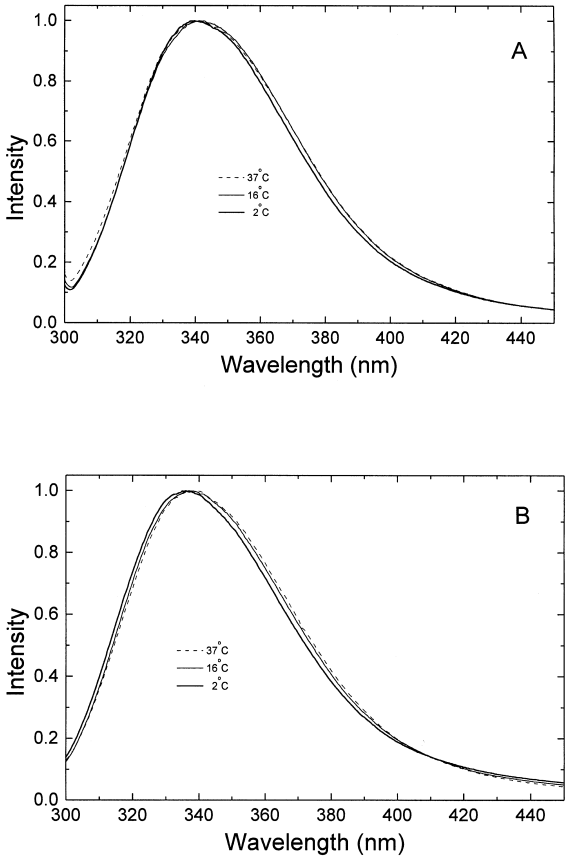

Fig. 1. Normalized emission spectra. (a) HSA in buffer; (b) HSA in glycerol/buffer. $\lambda_{ex} = 295$ nm (see also Sections 2.1 and 2.2).

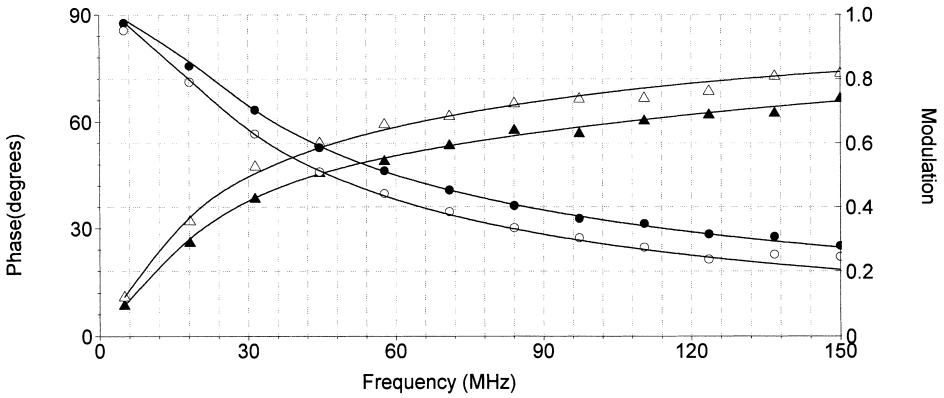

Fig. 2. Typical phase and modulation data measured at the blue side (325 nm, full signs) and the red side (380 nm, open signs) of the emission spectrum. Phase data: up triangles, modulation data: circles. HSA in buffer, $\lambda_{ex} = 295$ nm, $T = 0$°C (see also Sections 2.1 and 2.2).

data — lead to the suggestion that dielectric relaxation is the main reason of these effects. In the cases of either lower temperature or higher glycerol content the fluorescence emission originates from higher energy states, thus the steady-state spectra — reflecting an average of the total fluorescence emission — are relatively blue-shifted compared to spectra measured at higher temperatures and at lower glycerol content.

3.2. Dipolar relaxation of HSA

As an example Fig. 2 shows Φ phase and *m* modulation data directly measured by phase-fluorometer.

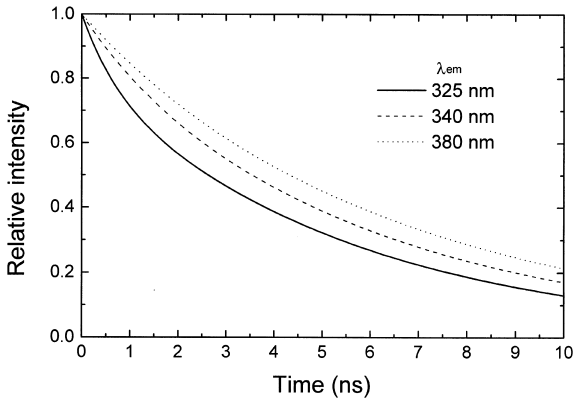

Fig. 3. Fluorescence decays of HSA in glycerol/buffer. $\lambda_{ex} = 295$ nm, $T = 6$°C (see also Sections 2.1 and 2.2).

From phase and modulation data the decay curves of fluorescence emission were constructed using 2–3 exponentials to fit (many times using three exponential components cannot give noticeable improvement compared to the two-exponential fit). Dielectric relaxation could be observable, if lifetimes of fluorescence emission and dielectric relaxation would not differ by orders of magnitude. The fluorescence decay slows down with increasing emission wavelength (Fig. 3) because the emission spectrum shifts toward a longer wavelength as a function of time.

To characterize the fluorescence decay with one parameter, one may choose the average fluorescence lifetime. As a result of time-dependent red-shift of the fluorescence emission spectrum the average fluorescence lifetime is shorter at the blue side and longer at the red side of the spectrum (Fig. 4).

Let us note that the average fluorescence lifetime (Fig. 4) increases when lowering the temperature, because the rate of non-radiative processes becomes lower. In the presence of glycerol the average fluorescence lifetime is lower (Fig. 5) (for comparison to NATA see Section 3.3).

Increasing the glycerol content of HSA solu-

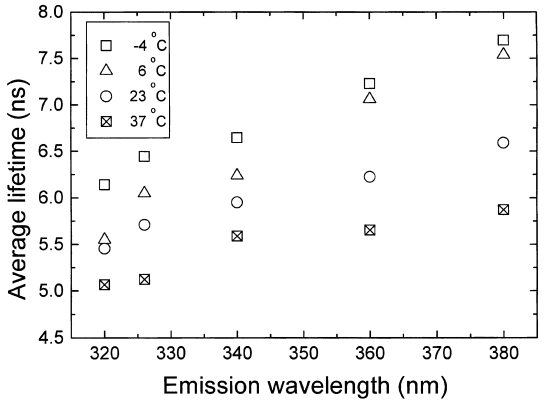

Fig. 4. Average fluorescence lifetime of HSA in glycerol/buffer as a function of emission wavelength and temperature. $\lambda_{ex} = 295$ nm (see also Sections 2.1 and 2.2).

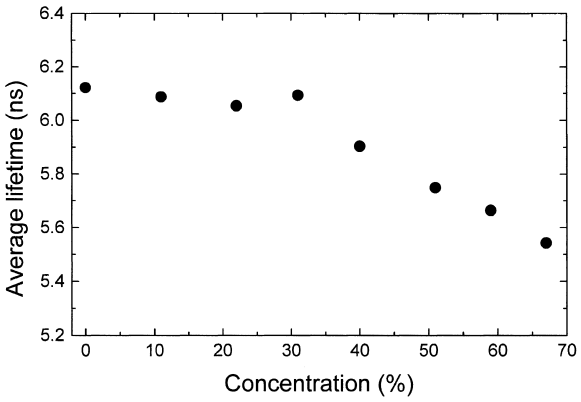

Fig. 6. Average fluorescence lifetime of total emission of HSA as a function of concentration of glycerol. $\lambda_{ex} = 295$ nm, $T = 23$°C (see also Sections 2.1 and 2.2).

tions (Fig. 6) the average fluorescence lifetime decreases when the glycerol content exceeds 30%.

This means that in the case of 50% glycerol — the concentration which was used in the present study — the local environment around the Trp residue of the HSA is changed already significantly. The Trp is more affected by the neighboring groups and the molecules of solvent — compared to the case of 0% glycerol — the rate of non-radiative processes is higher.

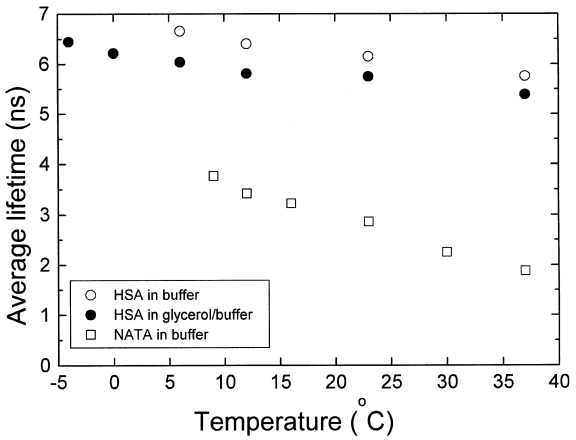

Fig. 5. Average fluorescence lifetime of total emission of HSA and NATA as a function of temperature. $\lambda_{ex} = 295$ nm (see also Sections 2.1 and 2.2).

Typical apparent fluorescence lifetimes are listed in Table 1. It is worth mentioning, that decay curves differing by not more than a few tenths of a percent from each other on the first 10-ns time-range can be created using two exponentials or a stretched exponential or even a double gaussian distribution of lifetime components. So one should be very careful when interpreting a good-looking fitting result. That is why we chose the simplest fitting function: the double exponential.

The total fluorescence is clearly not monoexponential. This fact — which is quite general in protein fluorescence — can be interpreted in terms of conformational substates. Already a little difference in the conformation of the fluorophore group could result in difference of rate of

Table 1
Typical apparent fluorescence lifetimes[a]

λ_{em} (nm)	a_1	a_2	τ_1 (ns)	τ_2 (ns)
325	0.80	0.20	5.52	0.69
330	0.86	0.14	5.75	1.06
340	0.87	0.13	6.13	1.46
350	0.91	0.09	6.32	1.36
360	0.93	0.07	6.45	1.30
370	0.93	0.07	6.49	1.26
380	0.94	0.06	6.79	2.10

[a] Two-component fits, HSA in 50% glycerol/buffer, $\lambda_{ex} = 295$ nm, $T = 6$°C. The error of lifetime data is ± 0.03 ns.

non-radiative processes, i.e. of the fluorescence lifetime. Finally, a non-monoexponential decay of total fluorescence can be measured. Let us keep in mind that the values for different wavelengths are only fitting parameters and not attributed as fluorescence lifetimes of different emitting species.

From the fluorescence decay curves the TEMs were constructed. Finally, $\bar{\nu}(t)$ mean wavenumbers were calculated, which describe the time-evolution of the dielectric relaxation.

The shape of the curves of Fig. 7 describes the decay of dielectric relaxation correctly in the first few nanoseconds. More or less this is the time-range where the intensity of fluorescence — the carrier of the dielectric relaxation — decreases to one-tenth of its starting value. Later, when the intensity of fluorescence becomes very low, the small differences in the longer lifetime components of the fittings of fluorescence decays will dominate and the move of $\bar{\nu}(t)$ in time shows artifacts.

The decays of DR can be fitted well (Fig. 8) by not more than two discrete exponentials in the first few nanoseconds (Table 2).

From the data of Table 2 it can be seen well, that the lower the temperature or the higher the viscosity of the solution is, the slower the DR is. The faster component is between 100 and 1000 ps, the longer one is between 3 and 10 ns. These two components appear in every DR decays reflecting two major steps in dielectric relaxation of HSA around Trp. Probably, both the faster and the slower phases of DR reflect a continuous redistribution within and between two groups of energetically close-lying metastable conformational substates [32]. Moreover, from simulations [33] the existence of even faster, sub-ps — ps components of DR are supposed.

As it was mentioned in Section 1, there are different explanations of the results of measurements. Generally, a negative pre-exponential factor of a fluorescence lifetime component considered to be an explicit appearance of an excited state reaction, as, e.g. DR [14]. It has to be emphasized, that this statement is true only in the case of monoexponential decay of the total fluorescence. In this case an apparent fast fluorescence decay component having positive pre-exponential factor appears at the blue side of the spectrum, and an apparent fast component having negative pre-exponential appears at the red side of the spectrum. When the total fluorescence itself has a double(or multi)-exponential decay then it is not sure at all that an apparent fluorescence decay component having negative pre-exponential factor would appear at the red side of the spectrum. It depends on the relative rates of fluorescence and DR decays. DR will result only in the change of pre-exponential factors and decay times of fluorescence of different emission wavelengths: the decay time components become longer and/or the longer components will have relatively higher pre-exponential factor values at

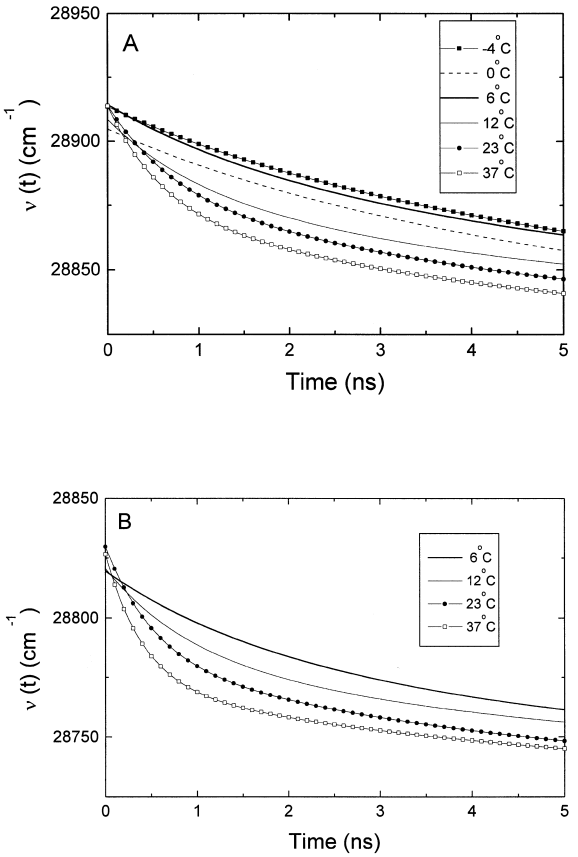

Fig. 7. Time evolution of $\bar{\nu}(t)$ mean fluorescence wavenumbers at different temperatures. (a) HSA in glycerol/buffer; (b) HSA in buffer. $\lambda_{ex} = 295$ nm (see also Sections 2.1 and 2.2).

Table 2
Decay parameters of DR[a]

Temperature (°C)		y_0 (cm^{-1})	a_1	a_2	t_1 (ns)	t_2 (ns)
37	Buffer	28 730	51.7	54.8	4.91	0.41
	Glycerol	28 820	52.3	41.4	5.43	0.61
23	Buffer	28 724	54.5	48.2	5.31	0.54
	Glycerol	28 822	56.6	35.3	5.94	0.74
12	Buffer	28 734	49.3	37.3	6.21	0.93
	Glycerol	28 827	52.4	29.1	6.73	1.03
6	Buffer	28 735	55.2	29.4	6.33	1.61
	Glycerol	28 832	63.9	18.4	6.85	1.53
0	Glycerol	28 819	78.4	9.4	7.41	1.71
−4	Glycerol	28 821	79.2	13.2	8.17	1.90

[a] $\nu(t) = y_0 + a_1 \cdot \exp(-t/t_1) + a_2 \cdot \exp(-t/t_2)$.

the red side compared to the values of these parameters of the blue side of the spectrum. These effects can be seen well in the data of Table 1. That is, the lack of a fluorescence decay component having negative pre-exponential is not evidence for the missing of DR.

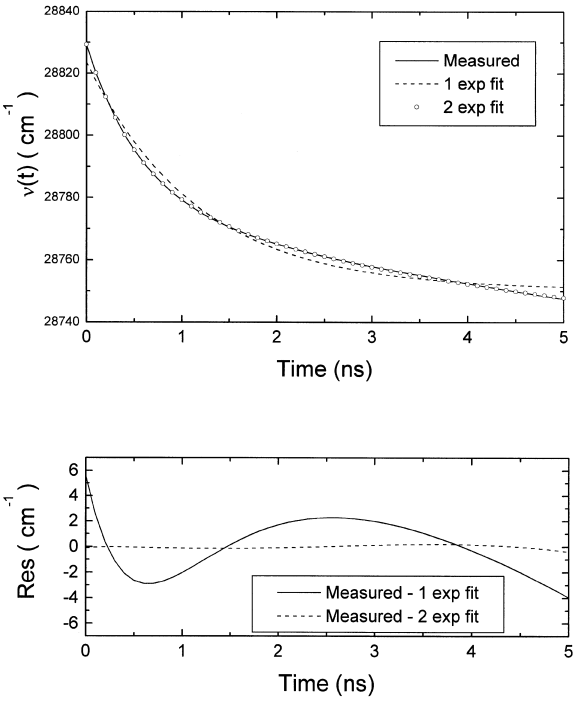

Fig. 8. Example for fits of $\bar{\nu}(t)$. Decay functions and residuals. HSA in buffer. $\lambda_{ex} = 295$ nm, $T = 23$°C (see also Sections 2.1 and 2.2).

3.3. Comparison to spectral characteristics of NATA

For comparison, the fluorescence properties of NATA were measured. Table 3 summarizes the fluorescence lifetimes of NATA at three different wavelengths.

The one-exponential fit for m and Φ data measured gives excellent results at all the temperatures studied. The temperature dependence of lifetime and intensity of total fluorescence of NATA are strongly correlated (Fig. 9).

The temperature dependence of lifetime of total fluorescence of NATA can be described with the following equation:

$$\tau(T) = \frac{1}{k_r + k_{nr}} = \frac{1}{k_r + k_{nr0} e^{-E_a/kT}}. \qquad (13)$$

Table 3
Fluorescence lifetimes of NATA. $\lambda_{ex} = 295$ nm[a]

λ_{em} (nm)	τ (ns) $T = 6$°C	τ (ns) $T = 23$°C
325	3.89	2.75
340	3.92	2.76
380	4.02	2.84

[a] The error of lifetime data is ±0.03 ns.

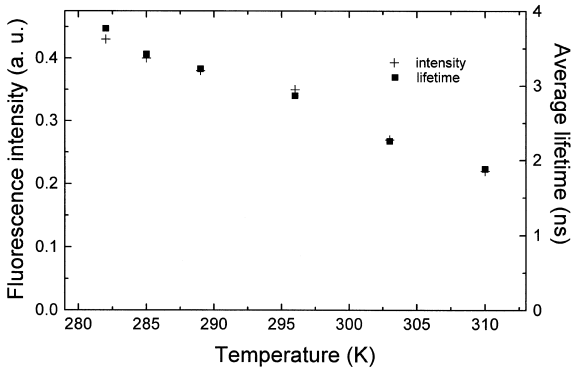

Fig. 9. Fluorescence intensity and average fluorescence lifetime of total emission of NATA as a function of temperature. $\lambda_{ex} = 295$ nm (see also Sections 2.1 and 2.2).

Fitting data of Fig. 9 yields $\tau_0 = 1/k_r = 20.8$ ns for the average natural lifetime of NATA.

Let us note, that a slight ($< 4\%$) increase of fluorescence lifetime can be found at the red side of the emission spectrum. A possible explanation of this effect might be that the radiative rate constant has a frequency dependence in the case of molecules with significant emission bandwidth.

From the lifetimes of Table 3 we should conclude that NATA does not show dielectric relaxation being in the sub-ns — ns time scale at the temperatures applied in our measurements. In contrast to this fact, the Trp emission of HSA has significant time-dependent Stokes shift. The reason is clearly the protein environment's influence on the Trp's emission.

4. Conclusions

Strong non-exponentiality of fluorescence decays of HSA was observed. From TEMs a time-dependent red shift of the emission spectra can be seen. These effects observed are explained by the presence of different conformational substates having different average fluorescence lifetimes and of DR of the protein environment of Trp residue. The rate of DR shows temperature dependence, which makes DR as a main mechanism probable. The composition of the solution also affects the rate of DR: the higher the glycerol content is, the slower the DR is. Besides slowing down the conformational motions of HSA, the glycerol changes the structures of the protein around the Trp residue, as well. Although the viscosity is the main parameter which is affected by the glycerol, a relatively small change of the dielectric constant and pH occurs, as well. Moreover, being a stabilizing agent, even larger concentrations do not alter the configuration of the native fold. However, increased stability of the protein by glycerol is achieved by inducing preferential hydration of the protein. To minimize the chemical potential, the HSA reduces its surface area by adopting more compact conformations [34]. In a more compact conformation HSA is believed to be more rigid.

As a result, the Trp is more influenced by its local protein and solvent environment. The rate of non-radiative processes becomes higher, that is the average fluorescence lifetime becomes lower. At the same time, DR became significantly slower according to the more compact conformations of the protein matrix.

Two major time-components of decay of DR are separated: a faster one between 100 and 1000 ps and a slower of approximately few nanoseconds. At the present quality of fluorescence decay measurements, the decay of DR can be fitted well with two exponentials in the first few nanosecond time region. The recovery of possible distribution of decay components of DR will need even more precise fluorescence decay measurements. We attribute these two, significantly different DR components to the different scale and different frequency motions of HSA [31,35].

Acknowledgements

This work was supported by grants from: National Technical Development Committee of Hungary No. OMFB 97-20-MU-0086, National Scientific Research Foundation No. OTKA 023209 and No. OTKA 032700, Project for Development of Research in Higher Education No. FKFP 0463/99.

References

[1] X. Song, D. Chandler, R.A. Marcus, Gaussian field model of dielectric solvation dynamics, J. Phys. Chem. 100 (1996) 11954–11959.

[2] E. Laitinen, K. Salonen, T. Harju, Solvation dynamics of 4-amino-*N*-methyl-phthalimide in *n*-alcohol solutions, J. Chem. Phys. 104 (1996) 6138–6148.

[3] E. Laitinen, K. Salonen, T. Harju, Solvation dynamics of 3-aminophthalimide in *n*-butanol solution at different temperatures, J. Chem. Phys. 105 (1996) 9771–9780.

[4] W.C. Flory, G.J. Blanchard, Excitation energy-dependent transient spectral relaxation, Appl. Spectrosc. 52 (1998) 82–90.

[5] C.P. Hsu, Y. Georgievskii, R.A. Marcus, Time-dependent fluorescence spectra of large molecules in polar solvents, J. Phys. Chem. A 102 (16) (1998) 2658–2666.

[6] T. Fonesca, B. Ladanyi, Breakdown of linear response for solvation dynamics in methanol, J. Phys. Chem. 95 (1991) 2116–2119.

[7] D.W. Pierce, S.G. Boxer, Dielectric relaxation in a protein matrix, J. Phys. Chem. A 96 (1992) 5560–5566.

[8] M.R. Eftink, C.A. Ghiron, Exposure of tryptophanyl residues and protein dynamics, Biochemistry 16 (25) (1977) 5546–5551.

[9] M. Eftink, Quenching-resolved emission anisotropy studies with single and multitryptophan-containing proteins, Biophys. J. 43 (1983) 323–334.

[10] S.T. Ferreira, Fluorescence studies of the conformational dynamics of parvalbumin in solution: lifetime and rotational motions of the single tryptophan residue, Biochemistry 28 (26) (1989) 10066–10072.

[11] L. Tilstra, M.C. Sattler, W.R. Cherry, M.D. Barkley, Fluorescence of a rotationally constrained tryptophan derivative, 3-carboxy-1,2,3,4-tetrahydro-2-carboline, J. Am. Chem. Soc. 112 (25) (1990) 9176–9182.

[12] K.J. Willis, A.G. Szabo, M. Zukker, J.M. Ridgeway, B. Alpert, Fluorescence decay kinetics of the tryptophyl residues of myoglobin: effect of heme ligation and evidence for discrete lifetime components, Biochemistry 29 (1990) 5270–5275.

[13] E.A. Permyakov, A.V. Ostrovsky, E.A. Burstein, P.G. Pleshanov, Ch. Gerday, Parvalbumin conformers revealed by steady-state and time-resolved fluorescence spectroscopy, Arch. Biochem. Biophys. 240 (2) (1985) 781–791.

[14] M. Vincent, J. Gallay, A.P. Demchenko, Dipolar relaxation around indole as evidenced by fluorescence lifetime distributions and time-dependence spectral shifts, J. Fluoresc. 7 (1) (1997) 107S–110S.

[15] K. Chu, R.M. Ernst, H. Frauenfelder, J.R. Mourant, G.U. Nienhaus, R. Philipp, Light-induced and thermal relaxation in a protein, Phys. Rev. Lett. 74 (13) (1995) 2607–2610.

[16] S.J. Kim, F.N. Chowdhury, W. Stryjewski, E.S. Younathan, P.S. Russo, M.D. Barkley, Time-resolved fluorescence of the single tryptophan of *Bacillus stearothermophilus* Phosphofructokinase, Biophys. J. 65 (1993) 215–226.

[17] N. Rosato, E. Gratton, G. Mei, A. Finazzi-Agro, Fluorescence lifetime distributions in human superoxide dismutase: effect of temperature and denaturation, Biophys. J. 58 (1990) 817–822.

[18] J.R. Lakowicz, H. Cherek, Dipolar relaxation in proteins on the nanosecond timescale observed by wavelength-resolved phase fluorometry of tryptophan fluorescence, J. Biol. Chem. 255 (3) (1980) 831–834.

[19] J.R. Alcala, E. Gratton, F.G. Prendergast, Fluorescence lifetime distributions in proteins, Biophys. J. 51 (1987) 597–604.

[20] J.R. Alcala, E. Gratton, F.G. Prendergast, Interpretation of fluorescence decays in proteins using continuous lifetime distributions, Biophys. J. 51 (1987) 925–936.

[21] J.R. Alcala, E. Gratton, F.G. Prendergast, Resolvability of fluorescence lifetime distributions using phase fluorometry, Biophys. J. 51 (1987) 587–596.

[22] A.P. Demchenko, J. Gallay, M. Vincent, H.-J. Apell, Fluorescence heterogeneity of tryptophans in Na,K-ATPase: evidences for temperature-dependent energy transfer, Biophys. Chem. 72 (1998) 265–283.

[23] K. Döring, L. Konermann, T. Surrey, F. Jähnig, A long lifetime component in the tryptophan fluorescence of some proteins, Eur. Biophys. J. 23 (1995) 423–432.

[24] A. Grinvald, I.Z. Steinberg, The fluorescence decay of tryptophan residues in native and denatured proteins, Biochim. Biophys. Acta 427 (1976) 663–678.

[25] W.B. de Lauder, Ph. Wahl, Fluorescence studies on human serum albumin, Biochem. Biophys. Res. Commun. 42 (1971) 398–402.

[26] R.F. Chen, V.J. Koester, Fluorescence properties of human serum albumin: effect of dialysis and charcoal treatment, Anal. Chem. 105 (1980) 348–353.

[27] B.D. Schlyer, J.A. Schauerte, D.G. Steel, A. Gafni, Time-resolved room temperature protein phosphorescence: nonexponential decay from single emitting tryptophans, Biophys. J. 67 (1994) 1192–1202.

[28] A. Vix, H. Lami, Protein fluorescence decay: discrete components or distribution of lifetimes? Really no way out of the dilemma? Biophys. J. 68 (1995) 1145–1151.

[29] J.R. Lakowicz, H. Cherek, I. Gryczynski, N. Joshi, M.L. Johnson, Analysisi of fluorescence decay kinetics measured in the frequency domain using distributions of decay times, Biophys. Chem. 28 (1987) 35–40.

[30] H.-T. Yu, M.A. Vela, F.R. Fronczek, M.L. McLaughlin, M.D. Barkley, Microenviromental effects on the solvent quenching rate in constrained tryptophan derivatives, J. Am. Chem. Soc. 117 (1) (1995) 348–357.

[31] X.M. He, D.C. Carter, Atomic structure and chemistry of human serum albumin, Nature 358 (1992) 209–215.

[32] S.J. Hagen, W.A. Eaton, Nonexponential structural relaxations in proteins, J. Chem. Phys. 104 (9) (1996) 3395–3398.
[33] T. Simonson, Ch.F. Wong, A.T. Brünger, Classical and quantum simulations of tryptophan in solution, J. Phys. Chem. A 101 (1997) 1935–1945.
[34] M. Gonelli, G.B. Strambini, Glycerol effects on protein flexibility: a tryptophan phosphorescence study, Biophys. J. 65 (1993) 131–137.
[35] W.G.J. Hol, L.M. Halie, C. Sander, Dipoles of the α-helix and β-sheet: their role in protein folding, Nature 294 (1981) 532–536.